

Enhanced Heat Transfer by Unipolar Injection of Electric Charges in Differentially Heated Dielectric Liquid Layer

Walid Hassen¹, Mohamed Naceur Borjini² and Habib Ben Aissia¹

Abstract: In this work we consider the problem related to the electro-thermo-convection of a dielectric fluid in a rectangular enclosure placed between two electrodes. This layer is subjected simultaneously to the injection of electric charges and to a thermal gradient. The influence of the electric Rayleigh number (200 - 1000) on the structure of the flow, the density of electric charge and heat transfer is investigated. An oscillatory flow is observed and discussed in detail.

Keywords: Heat transfer / Electro-Hydro-Dynamic (EHD) / Electro-thermo-convection / Dielectric liquid / Numerical simulation.

Nomenclature

a	Thermal diffusivity
t	Time
$C = \frac{q_0 \times L^2}{\epsilon_0 \times \Delta V}$	Dimensionless number which measure the injection strength
$T = \frac{\epsilon_0 \times \Delta V}{\rho \times \nu \times K_0}$	Electric Rayleigh number
E_x, E_y	Electric fields
U_x et U_y	horizontal and vertical velocity
g	acceleration of gravity
V	electric potential
H	Enclosure height
β	coefficient of thermal expansion
K_0	ionic mobility of the liquid
ϵ_0	permittivity of the fluid
L	Enclosure Width
θ	Temperature

¹ Ecole Nationale d'Ingénieurs, 5012 Monastir, Tunisia

² Corresponding author. Naceur.borjini@fsm.rnu.tn, Gsm 21698830979. Institut Supérieur des Sciences Appliquées et de Technologique, 4000 Sousse, Tunisia

$M = \frac{1}{K_0} \left(\frac{\epsilon_0}{\rho} \right)^{0,5}$	Dimensionless number which characterizes EHD properties of the liquid
θ_f et θ_c	Cold and hot wall temperature
Pr	Prandtl number
μ, ν	Dynamic and kinematic viscosity
q	Electric charge density
ρ	Density
$R = \frac{T}{M^2}$	Electric Reynolds number
Ψ	Stream function
$Ra = \frac{g \times \beta \times \Delta \theta \times L^3}{\nu \cdot \alpha}$	Thermal Rayleigh number
ω	vorticity

1 Introduction

The so-called “electro-thermo-convection” is an interdisciplinary subject associated with the interaction among fluids, heat transfer and electric fields [Castellanos (1998)].

In the last few years, such a phenomenon was well studied especially in dielectric liquids.

Indeed, it is well known today that the development of motion in a dielectric liquid layer between two electrodes (subjected to a high potential difference) is due to the action of the electric field on the electric charges injected into the liquid. One of the reasons which motivated the study of the Electro-Hydro-Dynamic (EHD) problem is that the development of instabilities in the liquid could be a promising way to increase the heat transfer using electric forces. As a natural consequence, the use of this technique may be used to reduce the size and cost of industrial heat exchangers. EHD phenomena also occur in several important industrial processes [Wong, Wang, Deval and Ho (2004)]. Indeed, new technologies in the field of micro-electro-mechanical and nanotechnology are strongly related to electro-thermo-convection [De Voe, Darabi and Ohadi (2001); Gonzalez, Green, Castellanos, Ramos and Morgan (2003)].

Most authors who worked so far on the EHD and on the electro-thermo-convection have mainly approached the resolution of this problem either experimentally or theoretically by stability analysis.

Atten, McCluskey and Perez (1987 and 1988) presented experimental studies with a Rayleigh-Bénard configuration. They showed that the agitation induced by the Coulomb force resulting from unipolar injection has a major influence on heat

transfer. Indeed, this transfer was increased by a factor ranging from 7 to 15 under their experimental conditions. They also tried to correlate the Nusselt number to the electric quantities (current of injection, electric potential) and to the geometry of field (distance separating the plans). They found a very satisfactory proportionality relationship. Similar results exist for unipolar charges injection in dielectric liquid lying between a wire and a coaxial cylinder [Atten and Elaouadie (1995)]. Also, stability of configuration with air/liquid two layer system under unipolar injection was studied by Koulova-Nenova, Atten and Elaouadie (1997).

For the case of non uniform electric field, Smorodin and Velarde (2001) and Takashima and Hamabata (1984) used electroconvective excitation to study the onset of instability in a differentially heated dielectric liquid subjected to an alternating electric field. They focused on the non-uniform polarization of the liquid, which was found to exert a negligible influence on the stability if the thermogravitationally-driven convection is strong.

Recently Vázquez, Georghiou and Castellanos (2006 and 2008) solved numerically the problem of isothermal electroconvection. Two different methods (*finite elements combined with the particle-in-cell method "FE-PIC"* and *finite elements and the flux-corrected transport method "FE-FCT"*) were tested, in particular. In the case of strong and weak injection, the structure of the flow and the distribution of the density of electric charge were examined resorting to a stability analysis technique.

Purely numerical works solving the coupled equations defining the problem are very rare in the literature. The first attempt carried out by Castellanos, Atten and Perez (1987) did not lead to satisfactory results, but recently Traoré, Koulova-Nenova, Romat and Perezc (2009) and Traoré, Perezc, Koulova-Nenova and Romat (2009 and 2010) could numerically determine the space-time evolution of the electro-thermo-convective flow.

In the present work, we solve numerically the entire set of equations associated with the electro-thermo-convective phenomena that take place in a planar layer of dielectric liquid differentially heated and subjected to unipolar injection. We focus essentially on the effect of the electric field on the flow structure and related heat transfer. Original results about oscillatory flow existing at relatively high values of the electric Rayleigh number are obtained.

2 Mathematical formulation and numerical model

We consider a layer of dielectric liquid confined in a square cavity of length L (Figure 1). The two vertical walls are maintained respectively at fixed temperatures θ_c et θ_f . On the two other adiabatic walls electrodes are placed. The emitter

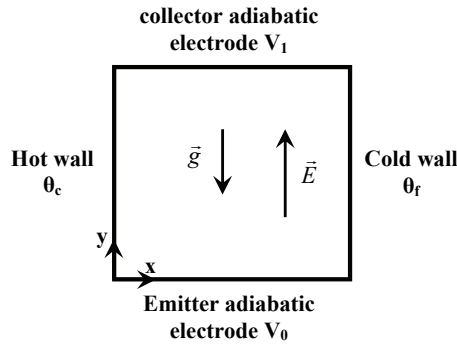


Figure 1: Geometry of enclosure

electrode corresponding to the plane $y=0$ is held at potential V_0 and is the source of ions which are injected into the liquid and collected by the electrode at $y=L$ which is held at potential V_1 .

The layer is thus subjected simultaneously to a thermal gradient $\Delta\theta = \theta_c - \theta_f$ and a potential difference $\Delta V = V_0 - V_1$.

Knowing that the electro-thermo-convection brings into play a variety of phenomena: hydrodynamic, thermal and electrical, the equations describing this problem take into consideration the following physical aspects:

The hydrodynamic aspects, including the equation of continuity and the equation of momentum (Navier-Stokes) containing force terms due to the internal viscosity, the gravity field and especially to electric force.

The thermal aspect is modelled by the equation of conservation of energy that takes into account the existence of the temperature gradient and the ensuing development of the natural convection phenomenon (this equation being coupled to the velocity field).

The electrical phenomenon that causes injection and migration of electric charges is described by the Gauss's theorem, by the equation of conservation of electric charges and by the relationship between the electric field and the electric potential V .

These equations under the Boussinesq assumption are written:

$$\nabla \cdot \vec{U}' = 0 \quad (1)$$

$$\rho_0 \left(\frac{\partial \vec{U}'}{\partial t'} + (\vec{U}' \cdot \nabla) \vec{U}' \right) = -\vec{\nabla} P' + \nabla \cdot (T^{visc} + T^{el}) + \rho \vec{g} \beta (\theta' - \theta_0) \quad (2)$$

$$\rho_0 C_p \left(\frac{\partial \theta'}{\partial t'} + \vec{U}' \cdot \nabla \theta' \right) = \nabla \cdot (\lambda \nabla \theta') \quad (3)$$

$$\frac{\partial q'}{\partial t'} + \nabla \cdot \vec{j} = 0 \quad (4)$$

$$\nabla \cdot (\epsilon \vec{E}') = q' \quad (5)$$

$$\vec{E}' = -\vec{\nabla} V' \quad (6)$$

With T^{visc} and T^{el} are the tensors of the forces of viscosities and the electric forces

$$\nabla \cdot T_{ij}^{visc} = \mu \left(\frac{\partial^2 U'_i}{\partial x'^2_j} + \frac{\partial^2 U'_j}{\partial x'^2_i} \right) \quad (7)$$

$$\nabla \cdot T^{el} = q\vec{E} - \frac{1}{2} E^2 \vec{\nabla} \epsilon_0 + \vec{\nabla} \left(\frac{1}{2} \rho E^2 \left(\frac{\partial \epsilon_0}{\partial q} \right)_\theta \right) \quad (8)$$

In equation (4) \vec{j} represents the density of electrical current which is equal according to [Atten and Moreau (1972)] and [Atten and Lacroix (1979)] to:

$$\vec{j} = q' \left(\vec{U}' + K \vec{E}' \right) \quad (9)$$

In equation (8) the first term known as Coulomb force, is the force per unit volume exerted by electric field on a medium containing free charges. Under D.C. conditions, the second term corresponds to the dielectric force and it is very weak compared to the Coulomb force.

The third term which represents the effect of electrostriction has the gradient form and can be absorbed in the pressure term of momentum equation but in the case of incompressible fluid (liquid) this term can be also neglected [Traoré, Koulova-Nenova, Romat, Perezc (2009); Ould El Moctar, Peerhossaini, Le Peurian and Bardon (1993); (1996); Atten and Moreau (1972); Paschkewitz and Pratt (2000)]. Thus the electric force can be expressed as:

$$\nabla \cdot T^{el} = q\vec{E} \quad (10)$$

As numerical method we had recourse to the “ Vorticity - Stream function” formalism ($\psi - \omega$), which allows the elimination of the pressure which is delicate to treat.

They are respectively defined by the two following relations:

$$\vec{\omega} = \nabla \times \vec{u} \quad (11)$$

$$\vec{u} = \nabla \times \vec{\psi} \quad (12)$$

Introducing the following dimensionless variables:

$$x = \frac{x'}{L} \quad y = \frac{y'}{L} \quad U_x = U'_x \frac{L}{a} \quad U_y = U'_y \frac{L}{a} \quad \psi = \frac{\Psi'}{a} \quad \omega = \omega' \frac{L^2}{a}$$

$$t = t' \frac{a}{L^2} \quad \theta = \frac{(\theta' - \theta_f)}{(\theta_c - \theta_f)} \quad q = \frac{q'}{q_0} \quad E = E' \frac{L}{(V_0 - V_1)} \quad V = \frac{(V' - V_1)}{(V_0 - V_1)}$$

For a two-dimensional geometry the system which governs this type of electro-thermo-convective flow (1) - (6) writes in adimensional form:

$$\omega = - \left(\frac{\partial^2 \Psi}{\partial x^2} + \frac{\partial^2 \Psi}{\partial y^2} \right) \quad (13)$$

$$\frac{\partial \omega}{\partial t} + U_x \frac{\partial \omega}{\partial x} + U_y \frac{\partial \omega}{\partial y} = \frac{\partial^2 \omega}{\partial x^2} + \frac{\partial^2 \omega}{\partial y^2} + Ra \cdot Pr \frac{\partial \theta}{\partial x} + \frac{CT^2}{M^2} \cdot Pr \left(\frac{\partial (qE_y)}{\partial x} - \frac{\partial (qE_x)}{\partial y} \right) \quad (14)$$

$$\frac{\partial \theta}{\partial t} + U_x \frac{\partial \theta}{\partial x} + U_y \frac{\partial \theta}{\partial y} = \left(\frac{\partial^2 \theta}{\partial x^2} + \frac{\partial^2 \theta}{\partial y^2} \right) \quad (15)$$

$$\frac{\partial q}{\partial t} + \frac{\partial}{\partial x} (q(U_x + R \cdot Pr \cdot E_x)) + \frac{\partial}{\partial y} (q(U_y + R \cdot Pr \cdot E_y)) = 0 \quad (16)$$

$$\frac{\partial^2 V}{\partial x^2} + \frac{\partial^2 V}{\partial y^2} = -C \cdot q \quad (17)$$

$$E_x = - \frac{\partial V}{\partial x} \quad (18)$$

$$E_y = - \frac{\partial V}{\partial y} \quad (19)$$

The associated initial and boundary conditions for the problem considered are as follows.

$$\text{For } t < 0: \omega = \Psi = \frac{\partial \Psi}{\partial y} = \frac{\partial \Psi}{\partial x} = \theta = V = q = 0 \text{ everywhere}$$

For $t > 0$

$$\text{Hot wall (x=0): } \Psi = \frac{\partial \Psi}{\partial y} = 0; \theta = 1; \frac{\partial q}{\partial y} = \frac{\partial V}{\partial y} = 0 \text{ et } \omega = - \frac{\partial^2 \Psi}{\partial x^2}$$

Cold wall ($x=L$): $\Psi = \frac{\partial \Psi}{\partial y} = 0$; $\theta = 0$; $\frac{\partial q}{\partial y} = \frac{\partial V}{\partial y} = 0$ et $\omega = -\frac{\partial^2 \Psi}{\partial x^2}$

Bottom wall ($y=0$): $\Psi = \frac{\partial \Psi}{\partial x} = 0$; $\frac{\partial \theta}{\partial y} = 0$; $q = 1$ et $V = 1$

Top wall ($y=L$): $\Psi = \frac{\partial \Psi}{\partial x} = 0$; $\frac{\partial \theta}{\partial y} = 0$; $\frac{\partial q}{\partial y} = 0$ et $V = 0$

Equations (13)–(19) are discretized using the control-volume method [Patankar (1980)]. The power-law scheme for treating convective terms and the fully implicit procedure to discretize the temporary derivatives are retained. The grid is uniform in both directions (51x51).

The resulting nonlinear algebraic equations are solved using the successive relaxation iterating scheme.

It is also noted that the adimensional parameters used for these simulations are: $Ra = 10\,000$, $Pr = 10$, $M = 10$ (corresponding to the liquid gas oil), $C = 10$ and T varies between 200 and 1000.

3 Validation tests

The results concerning the study of stability (critical electric Rayleigh) in the case of pure electrical problem (isothermal) are compared, in Table 1, to those yielded by Atten and Moreau (1972) for different injection level C .

Table 1: Variation according the injection level of the value of critical electric Rayleigh number

C	Critical T		Error (%)
	[15]	(présent work)	
0.5	1365.4	1359	0.47
0.7	821.5	823	0.18
1.4	351.3	352	0.2
2	258.5	257	0.58
2.8	211.2	210	0.56
3.5	192.6	191	0.83
5	175.7	174	0.97
7	167	165	1.19
10	164	160	2.44

Our results are in good agreement with those of Atten and Moreau (the error does not exceed 2.5%).

In order to test the electro-convective case coupled with heat transfer, we considered the conditions studied by Traoré, Perezc, Koulova-Nenova and Romat (2010),

i.e., an horizontal cavity, filled with a dielectric fluid, with a shape factor of 10 (the configuration adopted hence corresponds to Rayleigh-Bénard convection with unipolar injection from the bottom). In this situation the calculation is done with a mesh of 301 x 51. Figure 2 shows the variation of Nusselt number according to thermal Rayleigh number for several values of the electric Rayleigh number. We find that the results of our electro-thermo-convection model are in excellent agreement with Traoré et al. work since the error never exceeds 2%.

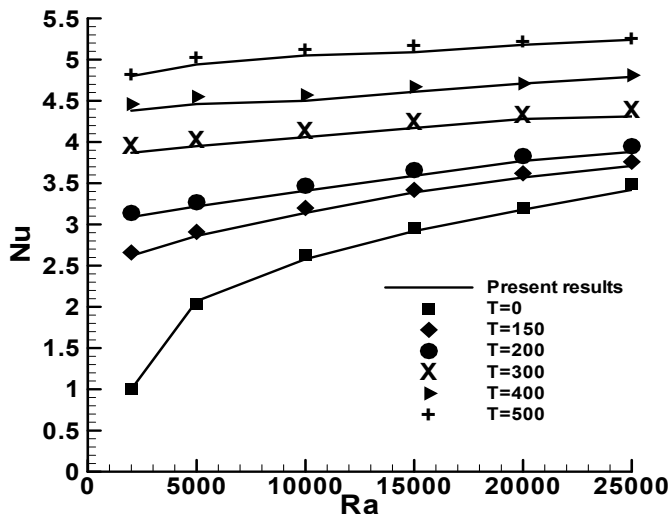


Figure 2: Variation of Nusselt number according to thermal Rayleigh number for several values of the electric Rayleigh number for $Pr=10$, $C=10$ and $M=10$.

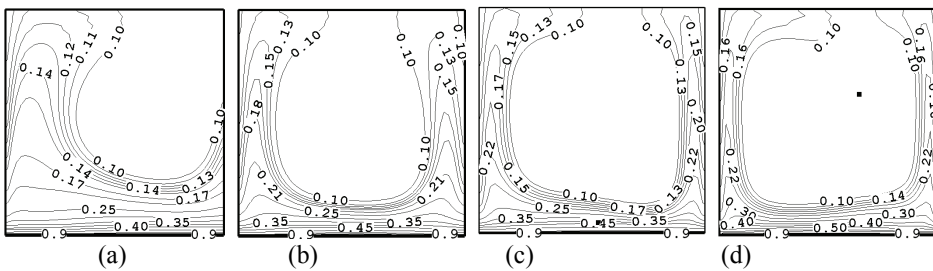


Figure 3: Isocontours of the electric charge density for $Pr=10$, $Ra=10^4$, $C=10$ and $M=10$

4 Results and discussion

4.1 Effect of the electric field on the density of charge

The distribution of the charge density shows that the greatest concentration of electric charge remains close to the bottom injecting wall, indeed this charge density drops by 50% after traversing only 3% length of the cavity. For a weak electric Rayleigh (figure 3 a) the electric charges migration reaches the top wall only from the side of the left hot wall.

By increasing the electric Rayleigh (figure 3 b, c and d) we observe that the charge migration takes place in the immediate vicinity of the two vertical walls. It is also noted that close to the top wall the charge density is more significant if the electric field is increased (table 2).

Table 2: Maximum charge density on the top wall

Electric Rayleigh	200	500	800	1000
Max q	0.11	0.14	0.15	0.16

4.2 Effect of the electric field on the structure of the flow

In the absence of electric field ($T = 0$, figure 4 a), the flow is driven by the thermal buoyancy force, so we obtain a large circulation buckle comprising a clockwise rotating single cell which occupies the entire cavity. We also note that the structure of the vortex has an elliptical shape in the longitudinal direction and its rotational speed is low. Starting the injection from the bottom electrode (Figure 4 b) it is clear that the electric and thermal fields are acting in the same direction. These latter fields engender a sudden acceleration of the rotation speed of the cell (which has almost doubled). The flow structure has not changed except the shape of the vortex becomes circular.

In the figure 4 c and d, the electric field is high enough that we notice the existence of a secondary counter rotating cell which appears and grows in the domain.

The first cell near the hot wall (left) is more impressive because it is due to the combination of both thermal and electrical forces (of Coulomb), while the second near the cold wall (right) is due to competition between the descending thermal force, and ascending Coulomb force, this competition promotes finally the electric force what allows the creation of this counter rotating cell.

By Further increasing the electric Rayleigh ($T = 1000$, figure 4 e), an unsteady flow is observed, indeed, a periodic oscillatory regime appears as can be seen in Figure 5.

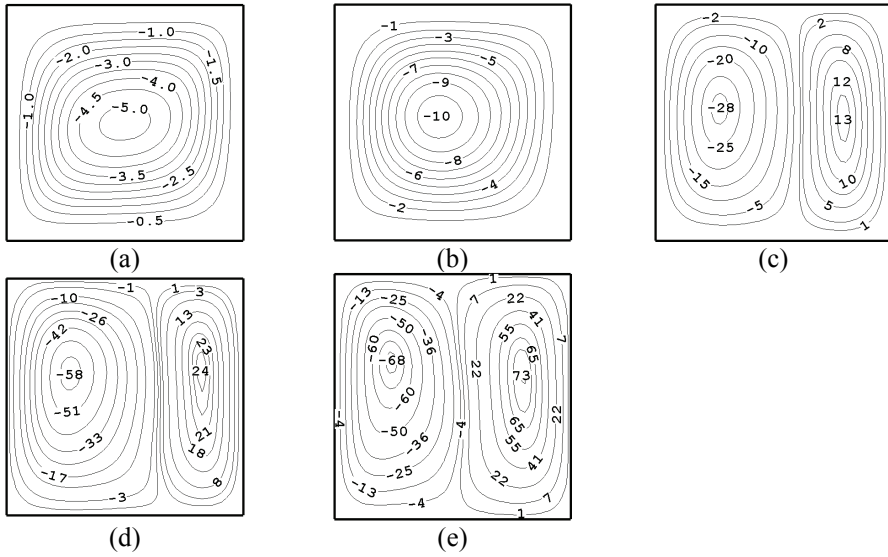


Figure 4: Representation of stream lines for $Pr = 10$, $Ra = 10^4$, $C = 10$ and $M = 10$. (a): $T = 0$; (b): $T = 200$; (c): $T = 500$; (d): $T = 800$; (e): $T = 1000$.

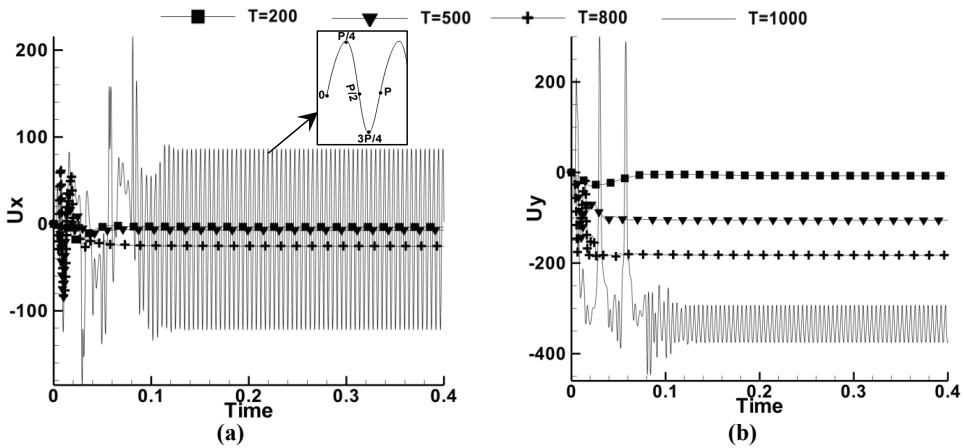


Figure 5: Temporal variations of velocity in the center of the cavity for $Pr = 10$, $Ra = 10^4$, $C = 10$ and $M = 10$

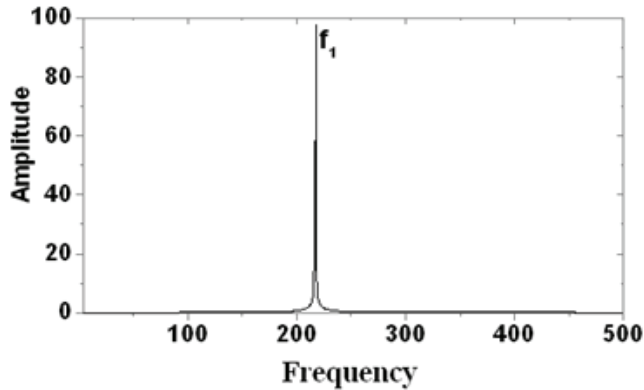


Figure 6: Spectrum of velocity amplitude in the center of the cavity for $Pr = 10$, $Ra = 10^4$, $C = 10$, $M = 10$ and $T = 1000$.

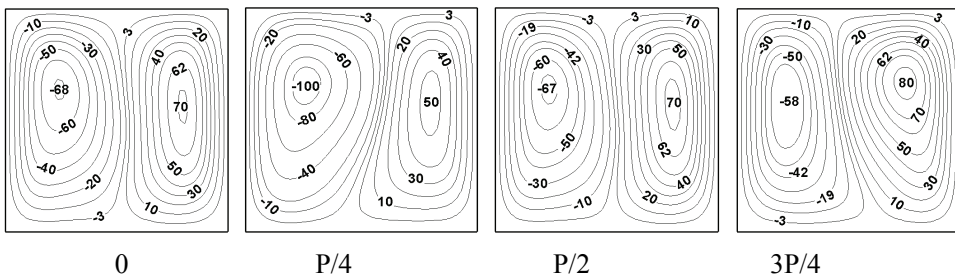


Figure 7: Streamline sequences during one main period (P) for $Pr = 10$, $Ra = 10^4$, $C = 10$, $M = 10$ and $T = 1000$.

The plot of the amplitude spectrum (Figure 6) confirms the existence of a fundamental frequency equal to $f_1 = 212$.

To study more profoundly the behavior of the flow during one period, Figure 7 illustrates a time sequence of streamlines over a period of oscillation (noted P) for $T = 1000$. On this figure we have during the period, two main cells against counter rotating on both sides of the center; we notice at the beginning of the period that the right cell is slightly more dominant. By advancing in the time it is the left cell which is growing and increases her rotation speed. So in half-period we have a dominant left cell and whose rotation speed is doubled compared to the other cell.

From $P/2$ it is the inverse phenomenon which begins i.e. the left cell loses the power in favor of the right cell what allows to return at the end of period to a

structure identical to that of the beginning.

This oscillatory regime is not due to the direct competition between the two out of phase thermal and coulombien forces. In fact similar oscillations are observed in pure electroconvection executions which may be explained by the phase shift between the charge density and the velocity disturbances [Pontiga, Castellanos (1994)]. This is partially approved in the works of Vázquez, Georghiou and Castellanos (2006, 2008). In reality the complex oscillatory two roll structure arises more from the coupling between the electric charge distribution and the velocity field than from non-linear components in the flow. The authors suggested also a simplified mechanism to understand the oscillations. In this scenario a virtual surface between charged region and void region expands with intensified velocity and inversely. This creates more liberated charges which drift more easily along the electric field. This mechanism remains valid for the present oscillatory electrothermo-convection flow.

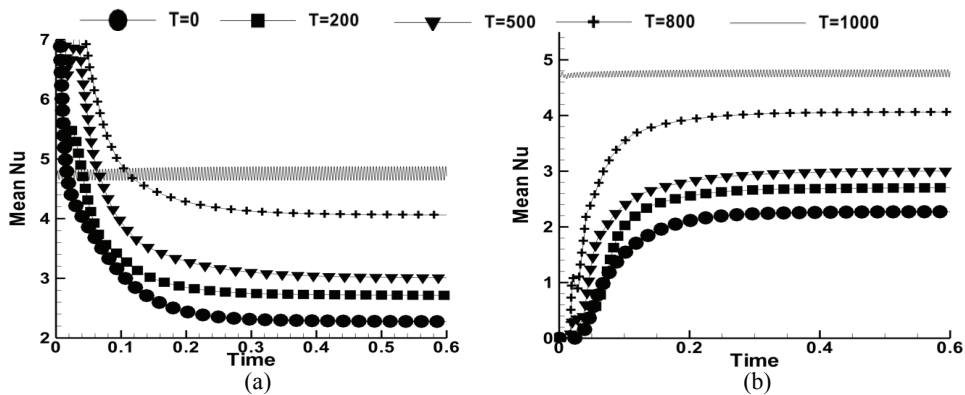


Figure 8: Time evolution of mean Nusselt number for $Ra=10^4$, $Pr=10$, $C=10$ and $M=10$

4.3 Effect of electric field on heat transfer

Figure 8 shows the time variation of mean Nusselt number for different values of the electric Rayleigh number. The charge injection increases significantly the value of the average Nusselt number compared to the case without injection. It is thus evident that heat transfer is increased by electrical activity in the flow. This increase in heat transfer compared to the case of classical natural convection is significant and it is summarized in Table 3.

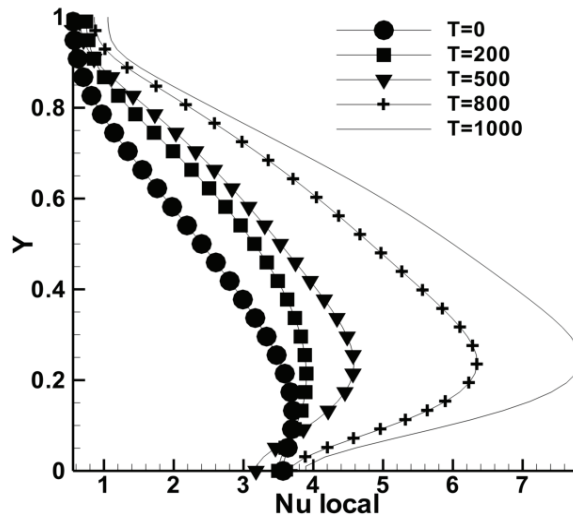


Figure 9: Variation of the local Nusselt number on the hot wall. ($Ra=10^4$, $Pr=10$, $C=10$ and $M=10$)

Table 3: Increase of the heat transfer according to the electric Rayleigh

Electric Rayleigh	200	500	800	1000
% of the increase	18%	32%	78%	112%

This increase in Nusselt number is directly related to dynamic mixing due to the swirling activity in the fluid. Whatever the value of the applied electric field, this mixing is increased significantly as seen clearly in Figure 4. All this is confirmed by Figure 9 which presents the local Nusselt number on hot wall. The examination of this figure shows the increase of local Nusselt number everywhere on the wall when the number of electric Rayleigh is more important.

5 Conclusion

In this work we have studied numerically the effect of unipolar injection of electric charges on the heat transfer in a layer of a dielectric liquid confined in a differentially heated square cavity. It has been shown that unipolar injection of electric charge by the bottom electrode changes in a radical way the topology of the thermo-convective flow. By increasing the mixing (induced by an electro-convective swirling activity), this injection amplifies the heat transfer significantly. For significant values of the electric Rayleigh number, an oscillatory regime occurs

and in these cases the heat transfer can be increased by 200%. This regime is principally set in motion by the coulomb force which plays the role of an amplifying and a restoring force at the same time as a consequence of the phase shift between the charge density and the velocity disturbances.

6 References

- Atten, P.; Elaouadie, L.** (1995): EHD convection in a dielectric liquid subjected to unipolar injection: Coaxial wire/cylinder geometry, *Journal of Electrostatics*, vol. 34, pp. 279-297.
- Atten, P.; Lacroix, J.C.** (1979): Non-linear hydrodynamic stability of liquids subjected to unipolar injection, *Journal of Mechanics*, vol. 18, pp. 469–510.
- Atten, P.; McCluskey, F.M.J.; Perez, A.T.** (1988): Electroconvection and its Effect on Heat Transfer, *IEEE Transactions on Electrical Insulation*, vol. 23, No. 4.
- Atten, P.; McCluskey, F.M.J.; Perez, A.T.** (1987): Augmentation du transfert thermique par électroconvection, *Revue Phys. Appl.*, vol. 22, pp. 1095-1101.
- Atten, P.; Moreau, R.** (1972): Stabilité électrohydrodynamique des liquides isolants soumis à une injection unipolaire, *Journal of Mechanics*, vol. 11, pp. 471–521.
- Castellanos, A.** (1998): *Electrohydrodynamics*. New York:Springer.
- Castellanos, A.; Atten, P.; Perez, A.T.** (1987): Finite amplitude electroconvection in liquid in the case of weak unipolar injection, *Physico-Chemical Hydrodynamics*, vol. 9 (3/4), pp.443–452.
- De Voe, D.L.; Darabi, J.; Ohadi, M.** (2001): An electrohydrodynamic polarization micropump for electronic cooling applications. *J. Microelectromech. Syst.*, vol. 10, pp 98-106
- Gonzalez, A.; Green, N.G.; Castellanos, A.; Ramos, A.; Morgan, H.** (2003): Electrohydrodynamics and dielectrophoresis in microsystems: *scaling laws*. *J. Phys. D: Appl. Phys.*, vol. 36, 2584–2597.
- Koulova-Nenova, D.; Atten, P.; Elaouadie, L.** (1997): EHD instability of air/liquid two layer system under unipolar charge injection, *Journal of Electrostatics*, 40-41, pp. 179-184.
- Ould El Moctar, A.; Peerhossaini, H.; Bardon, J.P.** (1996): Numerical and experimental investigation of direct electric conduction in a channel flow, *Int. J. Heat Mass Transfer*, Vol. 39, No. 5, pp. 975-993,
- Ould El Moctar, A.; Peerhossaini, H.; Le Peurian, P.; Bardon, J.P.** (1993): Ohmic heating of complex fluids, *Int. J. Heat Mass Transfer*, vol.36, pp. 3143-3152

- Paschkewitz, J.S.; Pratt, D.M.** (2000): The influence of fluid properties on electrohydrodynamic heat transfer enhancement in liquids under viscous and electrically dominated flow conditions, *Experimental Thermal and Fluid Science*, vol.21, pp. 187-197.
- Patankar, S.V.** (1980): *Numerical Heat Transfer and Fluid Flow*, McGraw–Hill, Washington, DC.
- Pontiga, F.; Castellanos, A.** (1994): Galerkin analysis of electrothermal instabilities in plane liquid layers, Industry Applications, *IEEE Transactions*, vol.30, pp. 862-876.
- Smorodin, B.L.; Velarde, M.G.** (2001): On the parametric excitation of electrothermal instability in a dielectric liquid layer using an alternating electric field, *Journal of Electrostatics*, vol. 50/3, pp. 205-226.
- Takashima, M.; Hamabata, H.** (1984): The stability of natural convection in a vertical layer of dielectric fluid in the presence of a horizontal ac electric field, *J. Phys. Soc. Jpn.*, vol.53, pp. 1728-1736.
- Traoré, Ph.; Perez, A.; Koulova-Nenova, D.; Romat, H.** (2010): Numerical modelling of finite-amplitude electro-thermo-convection in a dielectric liquid layer subjected to both unipolar injection and temperature gradient, *J. Fluid Mech*, vol. 658, pp. 279–293.
- Traoré, Ph.; Koulova-Nenova, D.; Romat, H.; Perez, A.** (2009): Caractérisation de l'augmentation des transferts thermiques dans une couche de liquide diélectrique soumise à une injection unipolaire de charges électriques, *C. R. Mécanique*, vol. 337, pp.150–157.
- Traoré, Ph.; Perez, A.; Koulova-Nenova, D.; Romat, H.** (2009): Analyse par simulation numérique du développement de l'instabilité électro-convective d'une couche de liquide diélectrique infinie soumise à une injection unipolaire, *C. R. Mécanique*, vol. 337, pp. 667–674.
- Vázquez, P.A.; Georghiou, G.E.; Castellanos, A.** (2006): Characterization of injection instabilities in electrohydrodynamics by numerical modelling: comparison of particle in cell and flux corrected transport methods for electroconvection between two plates, *J. Phys. D: Appl. Phys.*, vol. 39, pp. 2754 – 2763.
- Vázquez, P.A.; Georghiou, G.E.; Castellanos, A.** (2008): Numerical analysis of the stability of the electrohydrodynamic (EHD) electroconvection between two plates, *J. Phys. D: Appl. Phys.*, vol. 41, 175303.
- Wong, P.K.; Wang, T.H.; Deval, J.H.; Ho, C.M.** (2004): Electrokinetics in micro devices for biotechnology applications. *IEEE/ASME Trans. Mechatro*, 9366 – 9376.

